Available online at www.sciencedirect.com

SciVerse ScienceDirect

Ceramics International 39 (2013) 2883–2887

CERAMICS INTERNATIONAL

www.elsevier.com/locate/ceramint

C_2H_2 gas sensor based on Ni-doped ZnO electrospun nanofibers

Xinchang Wang[a,*], Minggang Zhao[a], Fang Liu[a], Jianfeng Jia[a], Xinjian Li[a], Liangliang Cao[b]

[a]Key Laboratory of Material Physics Ministry Education, and School of Physics and Engineering, Zhengzhou University, Zhengzhou 450052, PR China
[b]nGimat Co., Atlanta, GA 30341, USA

Received 29 August 2012; received in revised form 17 September 2012; accepted 20 September 2012
Available online 28 September 2012

Abstract

Pure and Ni-doped ZnO nanofibers were synthesized using the electrospinning method. The morphology, crystal structure and optical properties of the nanofibers were characterized by scanning electron microscopy (SEM), X-ray diffraction (XRD) and photoluminescence (PL) spectroscopy, respectively. It is found that Ni doping does not change the morphology and crystal structures of the nanofibers, and the ultraviolet emissions of ZnO nanofibers present red shift with increasing Ni doping concentration. C_2H_2 sensing properties of the sensors based on the nanofibers were investigated. The results show that the C_2H_2 sensing properties of ZnO nanofibers are effectively improved by Ni doping, and 5 at% Ni-doped ZnO nanofibers exhibit a maximum sensitivity to C_2H_2 gas.

Keywords: Ni-doped ZnO; Nanofiber; Gas sensor; C_2H_2

1. Introduction

ZnO, an important semiconductor material with a large binding energy (60 meV) and a wide band gap (3.37 eV), has attracted considerable interests in view of its remarkable optoelectronic properties and the sensitivity to various gases, all of which make ZnO highly promising in a broad range of real-world applications [1,2]. Recently, ZnO has shown great potentials for sensing toxic and combustible gases such as CO, H_2, NH_3, C_2H_5OH and H_2S [3–7], whereas some inherent drawbacks including low sensitivity, high working temperature and restricted detection of low concentration gases, may hinder the further development of ZnO-based sensors.

To solve these problems, two methods, introducing specific dopants or increasing the surface-to-volume ratio of the building materials [8–10], have been generally believed to be able to improve the performance of the ZnO-based gas sensors. Various metal elements such as Al and Pt have been tried as the dopant into ZnO for enhancing the sensing properties, and some promising results have been achieved [11,12]. In addition, numerous nanostructures, including nanowires [13], nanosheets [14], nanoparticles [15] as well as nanofibers [16], have been synthesized for further increasing the surface-to-volume ratio of ZnO materials, and various methods for nanomaterials synthesis have also been explored, such as chemical vapor deposition, template-based growth, solution and electrospinning [13–17]. Among these methods, electrospinning has been proved to be a versatile, effective, simple and inexpensive method to fabricate 1D nanofibers with high specific surface area, arising from their rough surface and large surface-to-volume ratio, both of which make the nanofibers highly competitive for making the novel nanomaterials-based gas sensors [18,19]. Recently, the fabrication and sensing properties of electrospun ZnO nanofibers doped with proper elements such as Cu, Co and Pd have been reported [20–22]. However, the sensing properties of Ni-doped ZnO nanofibers have been rarely investigated.

In this work, we report the synthesis and gas sensing properties of pure and Ni-doped ZnO nanofibers through the electrospinning technique. The sensor fabricated from Ni-doped ZnO nanofibers exhibits improved C_2H_2 sensing properties. The results show that Ni-doped nanofibers are very promising materials for fabricating high performance C_2H_2 sensors.

*Corresponding author. Tel.: +86 371 67766917.
E-mail address: wxclhm@zzu.edu.cn (X. Wang).

0272-8842/$ - see front matter © 2012 Elsevier Ltd and Techna Group S.r.l. All rights reserved.
http://dx.doi.org/10.1016/j.ceramint.2012.09.062

2. Experimental

Ni-doped ZnO nanofibers with different doping concentrations were prepared by electrospinning. In a typical procedure, the same amount of zinc acetate (2.19 g) and various amount of Ni $(NO_3)_2$ were added into 30 ml of the as-prepared polyvinyl alcohol (PVA, Mw 80,000) aqueous solutions (10 wt%) with stirring, and the reaction proceeded at 50 °C for 1 h. This mixture was aged at room temperature for 4 h, and then the viscous sol solution was obtained as the precursor for the following electrospinning process.

The precursor solutions were electrospun at the positive voltage of 8 kV and a tip-to-collector distance of 20 cm at room temperature to form the nanofibers, which was collected on a grounded substrate, and then were calcined at 650 °C for 3 h in air to remove the organic moiety. The morphology, composition and crystal structure of the as-prepared nanofibers were characterized with scanning electron microscopy (SEM), energy dispersive X-ray (EDX) spectroscopy and X-ray diffraction (XRD), respectively. Room temperature photoluminescence (PL) spectroscopy with He–Cd (325 nm) laser lines as the excitation sources was used to examine the optical properties of the nanofibers.

The as-prepared ZnO nanofibers were mixed with a suitable amount of deionized water to form a paste, which was coated onto a ceramic tube with a pair of Au electrodes and Pt wires on both ends. A heating coil through the tube was employed to adjust the operating temperature of the sensors. After drying and aging, the nanostructured coating was formed, and the sensors were ready for use. A static test system was adopted for testing, where the performance of the gas sensors was tested in a closed chamber with a volume of 18 L, and the target gas was injected into the chamber by a syringe. In this present paper, the gas sensitivity was defined as $S = R_a/R_g$, where R_g and R_a are the resistances of samples with and without the presence of the detected gas, respectively. The response and recovery time was defined as the time taken for the sensor to reach 90% of the total resistance change in the presence (target gas adsorption) and in the absence (target gas desorption) of the detected gas in a step function.

3. Results and discussion

Fig. 1(a) and (b) shows the SEM images of the as-fabricated pure and 5 at% Ni-doped ZnO nanofiber mats, respectively, both of which exhibit a similar two-level nanostructure. Firstly, the nanofibers, with the length up to several millimeters and the diameter about 100 nm, are randomly distributed and form a fibrous nonwoven mat. Secondly, as shown in the enlarged image (the inset images of Fig. 1(a) and (b)), the single nanofiber is composed of another sub-level nanostructures, about 25–50 nm in size, which makes the surface of the nanofiber considerably rough and full of void space. Obviously, such hierarchical structures provided by the electrospun nanofibers can significantly enhance the surface-to-volume ratio of the sensing materials, and thus, may contribute to the gas diffusion and mass transport in the materials so as to improve the performance of the resulting sensors.

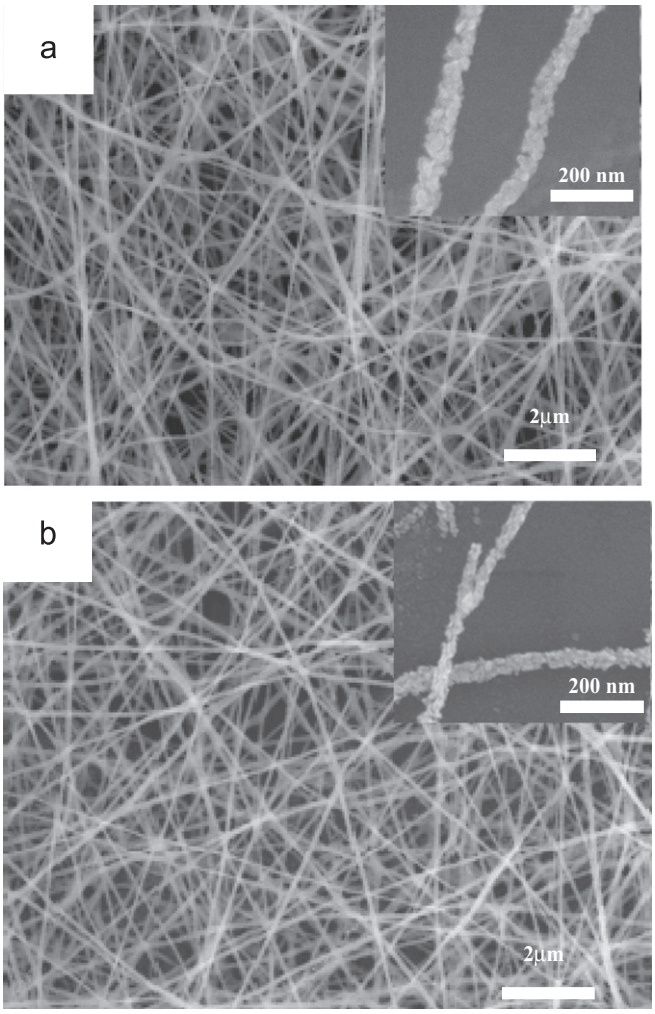

Fig. 1. SEM images of pure (a) and 5 at% Ni-doped (b) ZnO nanofibers calcined at 650 °C for 3 h.

X-ray diffraction (XRD) was used to examine the effect of Ni doping on the crystal structure of the ZnO nanofibers. As shown in Fig. 2(a), all the diffraction peaks can be indexed as hexagonal ZnO crystal structure for both undoped and 5 at% Ni-doped ZnO nanofibers, and the good sharpness of the peaks reveal a highly crystallized wurtzite structure. With regard to the Ni-doped nanofibers, no peaks corresponding with Ni or NiO are observed, indicating that doping Ni has no apparent effect on the crystal structures of the ZnO nanofibers, whereas the (101) peak position shifts from 36.08° to 36.24°, implying that the lattice constant of ZnO crystal has somewhat changed, where Ni impurities would be in the form of Ni^{2+} ions and partly substituted the Zn^{2+} sites in the lattice [23]. The EDX pattern of 5 at% Ni-doped ZnO nanofibers shown in Fig. 2(b) reveals the presence of Zn, O, Ni and Si elements (Si peaks come from Si substrate), and no impurity elements including carbon are clearly observed, indicating that the carbon element originating from PVA has been

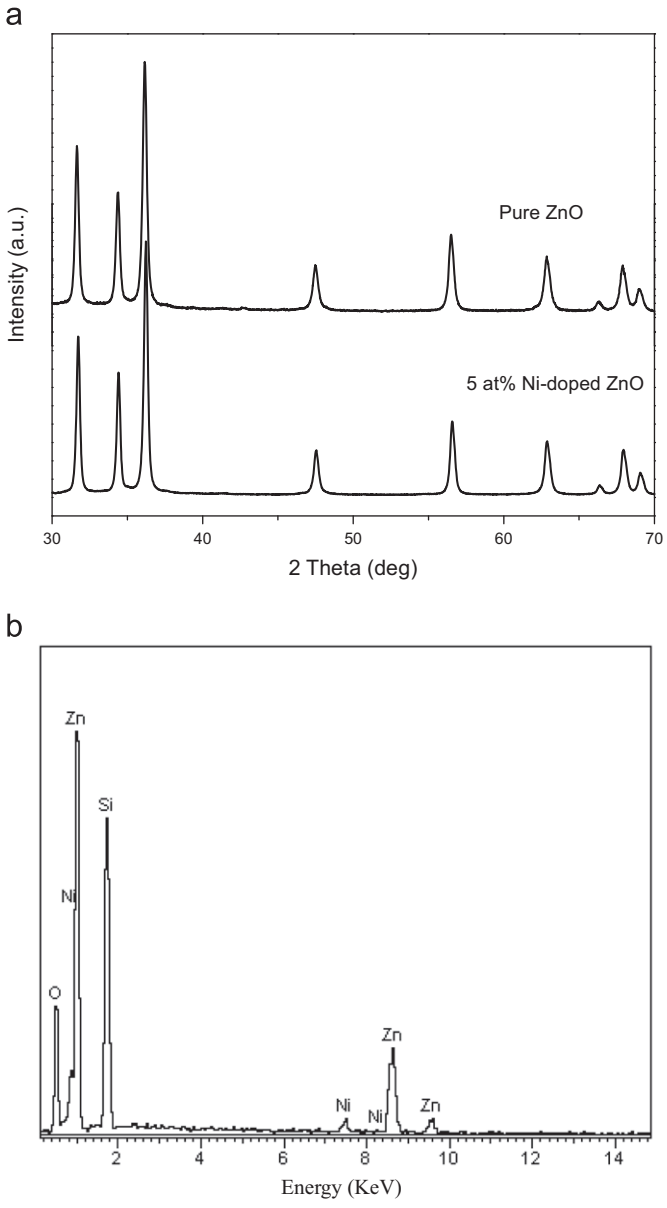

Fig. 2. (a) XRD patterns of pure ZnO and 5 at% Ni-doped ZnO nanofibers calcined at 650 °C for 3 h. (b) EDX spectra of 5% Ni-doped ZnO nanofibers.

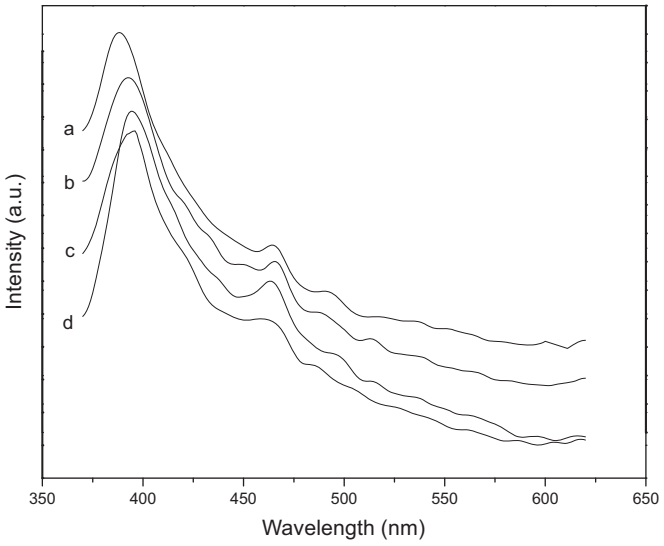

Fig. 3. Room temperature photoluminescence spectrum of Ni-doped ZnO nanofibers with different doping concentrations after calcinations: (a) 0; (b) 3; (c) 5 and (d) 8 at%.

fully removed during the heating treatment in air. The Ni content is determined to be about 5 at% for the nanofibers, which is close to the theoretical value. The patterns of 3 at% and 8 at% Ni-doped ZnO nanofibers are similar to the results in Fig. 2(b).

Fig. 3 shows the PL spectra of Ni-doped ZnO nanofibers with different doping concentrations. Two peaks are observed in all samples, an ultraviolet (UV) emission (around 390 nm) originating from the exciton recombination of ZnO [24], and a blue emission peak (around 465 nm) arising from the intrinsic defects in the ZnO nanofibers such as the Zn interstitials and the oxygen vacancies-related donor defects [25]. With gradually increasing the Ni doping concentration, the peak position of UV emission peak exhibits red shift from 387 nm to 396 nm because of the modulation of the band-gap caused by Ni substitution, which indicates that the optical band-gap (E_g) of the Ni-doping ZnO nanofibers can be tunable by changing the Ni doping concentration. This may be explained by the crystal lattice confinement effect [26]. The doped Ni^{2+} enters into the ZnO crystal structure, and forms the localized band edge states with a reduced E_g. The blue emission, on the other hand, becomes stronger as doping more Ni into the ZnO nanofibers, and eventually reaches the maximum value when the Ni doping concentration was 5 at%, but then decreased. This result reveals that Ni doping can facilitate the formation of the intrinsic defects, either Zn interstitials or oxygen vacancies, so as to increase the density of the blue emission.

The gas-sensing properties of Ni-doped ZnO nanofibers to C_2H_2 were investigated. Fig. 4 shows the sensitivities of pure and Ni-doped ZnO nanofibers to 2000 ppm C_2H_2 gas at different operating temperatures. The sensitivities of all samples are found to increase with increasing the operating temperature, which attain the maximum at 250 °C, and then decrease with a further rise of the operating temperature. It is believed that there is a potential barrier for charge transport formed during adsorption of atmospheric oxygen molecules on the surface, which prevents the C_2H_2 molecules from reacting with the surface adsorbed oxygen species at low temperatures. When the temperature was raised up to 250 °C, the C_2H_2 molecules were provided with sufficient energy to overcome the barrier, and hence, the chemical reactions occurring on the surfaces were facilitated, resulting in a remarkably decreased R_g so as to enhance the sensitivity. When the temperature was higher than 250 °C, the sensitivity was continuously reduced, which may result from the decrease of the adsorbed oxygen species available at the sensing sites on the surface for reaction and the increase in intrinsic sensor resistance in air [27]. Moreover, we can also find that all of Ni-doped ZnO nanofibers show higher sensitivities to C_2H_2 than the pure

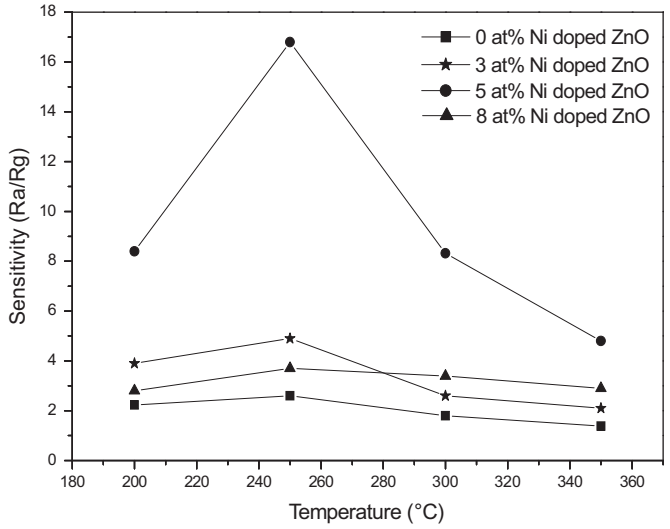

Fig. 4. Sensitivity of pure and Ni-doped ZnO nanofibers to 2000 ppm C_2H_2 gas at various operating temperatures.

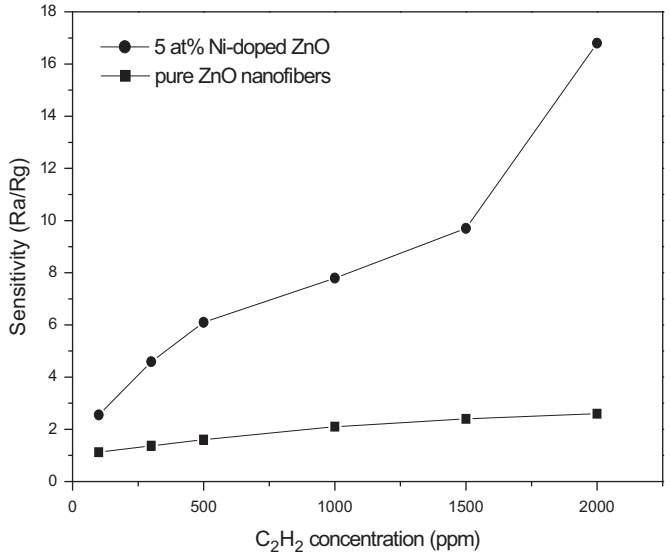

Fig. 5. Sensitivities of sensors upon different C_2H_2 gas concentrations at 250 °C.

ZnO nanofibers, and the sensitivity increases up to 5 at% Ni-doped ZnO nanofibers, but the samples with the excess Ni concentration such as 8 at% deteriorate with worse sensitivity (as shown in Fig. 4). At the optimal Ni doping concentration (8 at%), the sensitivity of the gas sensor can reach the maximum values (16.9), which is 6.5 times larger than that of pure ZnO nanofibers (2.6). The results suggest that Ni doping is the effective method in improving the sensing performance of the ZnO nanofibers-based sensor, and the optimal Ni doping concentration is 5 at%.

Fig. 5 shows the response characteristics of the nanofibers as a function of C_2H_2 concentration in air at the operating temperature of 250 °C. As observed, the response of the nanofibers increased with the increasing concentration of C_2H_2. The Ni-doped ZnO nanofibers had a more rapid increase than the pure. The response and recovery times were showed in Fig. 6. We can see that both samples exhibited fast response after C_2H_2 was injected, and reached to the equilibrium value about 5 s. The signal decreased as the acetylene gas was pumped out and came back to the initial value within 10 s. The fast response and recovery time might be attributed to the 1D nanostructures of the nanofibers, which facilitated the fast mass transfer of C_2H_2 molecules to and from the interaction region as well as improved the rate for charge carriers to traverse the barriers induced by molecular recognition along the nanofibers [28,29].

It is well accepted that the gas-sensing mechanism of ZnO-based sensors belongs to surface-controlled type, namely, the sensitivity is attributed to the chemisorption of oxygen on the oxide surface and the subsequent reaction between adsorbed oxygen and test gas, which brings the resistance change. Prior to the test gas (C_2H_2) injection, the oxygen molecules in air will absorb on the fiber surface to generate chemisorbed oxygen species (O_2^-, O^{2-} and O^-) by capturing electrons from the ZnO conduction band. Consequently, ZnO will show a high resistance. Takata et al. found that the chemisorbed oxygen species depend strongly on temperature, and the stable oxygen ions were O_2^- below 100 °C, O^- between 100 and 300 °C, and O^{2-} above 300 °C [30]. Since the sensor was operated at 250 °C, the O^- species were more important than other oxygen adsorbates. When Ni-doped ZnO is exposed to reductive gases (C_2H_2), the C_2H_2 molecules will react with adsorbed O^- species on the ZnO surface to form CO_2 and H_2O, which leads to the increase of carrier concentration and the decrease of the electrical resistance. On the basis of the discussion, the C_2H_2 sensing mechanism of this ZnO-based gas sensor may be described as follows:

$$O_2(gas) + 2e^- \rightarrow 2O_{ads}^-$$

$$C_2H_2(ads) + 5O_{ads}^- \rightarrow 2CO_2 + H_2O + 5e^-$$

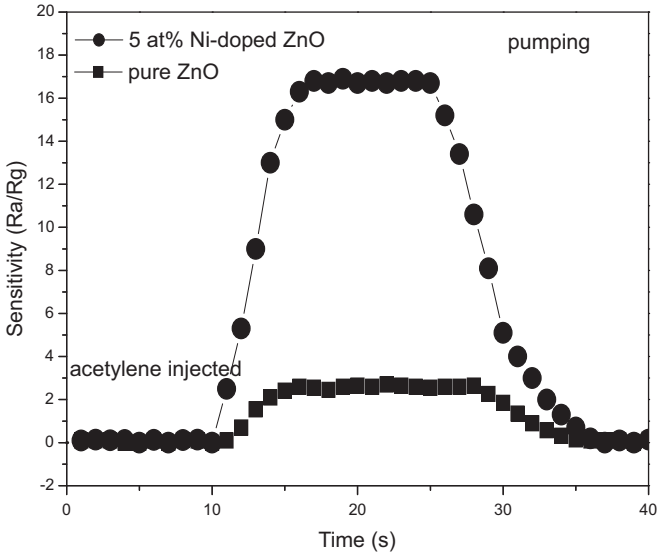

Fig. 6. Response-recovery characteristics of the sensors based on pure and 5 at% Ni-doped ZnO nanofibers to 2000 ppm C_2H_2 gas at 250 °C.

The high performance of our nanofibers is also up to the sensing improvement brought by Ni doping. By doping Ni in ZnO, impurity energy levels will be introduced, and the degree of releasing trapped electrons will be greater than that without doping, which will result in greater degree of resistance decrease. Therefore, the gas sensing properties of ZnO nanofibers are improved.

4. Conclusion

In summary, pure and Ni-doped ZnO nanofibers were successfully synthesized by a simple electrospinning method. The hexagonal ZnO nanofibers with diameters about 100 nm had characteristic morphology and large aspect ratio. The room temperature PL measurements indicate that Ni doping can facilitate the formation of the intrinsic defects and influence the band gap of ZnO. The C_2H_2 sensing measurements show that the response to C_2H_2 gas has been greatly enhanced by Ni doping, and the optimal doping concentration was 5 at%.

Acknowledgments

The authors gratefully acknowledge the financial support of the Foundation for University Middle-aged Key Teacher by Henan Province (Grant no. 2010GGJS-001) and the Technology Project on Key Problems of Henan Province (Grant no. 082101510007).

References

[1] M.H. Huang, S. Mao, H. Feick, H.Q. Yan, Y.Y. Wu, H. Kind, E. Weber, R. Russo, P.D. Yang, Room-temperature ultraviolet nanowire nanolasers, Science 292 (2001) 1897–1899.

[2] S.H. Choi, G. Ankonina, D.Y. Youn, S.G. Oh, J.M. Hong, A. Rothschild, I.D. Kim, Hollow ZnO nanofibers fabricated using electrospun polymer templates and their electronic transport properties, ACS Nano 3 (2009) 2623–2631.

[3] Y. Zhang, J.Q. Xu, Q. Xiang, H. Li, Q.Y. Pan, P.C. Xu, Brush-like hierarchical ZnO nanostructures: synthesis, photoluminescence and gas sensor properties, Journal of Physical Chemistry C 113 (2009) 3430–3435.

[4] S.S. Badadhe, I.S. Mulla, H_2S gas sensitive indium-doped ZnO thin films: preparation and characterization, Sensors and Actuators B 143 (2009) 164–170.

[5] A.K. Bai, A. Singh, R.K. Bedi, Characterization and ammonia sensing properties of pure and modified ZnO films, Applied Physics A 103 (2011) 497–503.

[6] O. Lupan, W. Ursaki, G. Chai, L. Chow, G.A. Emelchenko, I.M. Tiginyanu, A.N. Gruzintsev, A.N. Redkin, Selective hydrogen gas nanosensor using individual ZnO nanowire with fast response at room temperature, Sensors and Actuators B 144 (2010) 56–66.

[7] S.K. Youn, N. Ramgir, C.Y. Wang, K. Subannajui, V. Cimalla, M. Zacharias, Catalyst-free growth of ZnO nanowire based on topographical confinement and preferential chemisorption and their use for room temperature CO detection, Journal of Physical Chemistry C 114 (2010) 10092–10100.

[8] P.P. Sahay, R.K. Nath, Al-doped ZnO thin films as methanol sensors, Sensors and Actuators B 134 (2008) 654–659.

[9] F. Gyger, M. Hübner, C. Feldmann, N. Barsan, U. Weimar, Nanoscale SnO_2 hollow spheres and their application as a gas-sensing material, Chemistry of Materials 22 (2010) 4821–4827.

[10] D.J. Yang, I. Kamienchick, D.Y. Youn, A. Rothschild, I.D. Kim, Ultrasensitive and highly selective gas sensors based on electrospun SnO_2 nanofibers modified by Pd loading, Advanced Functional Materials 20 (2010) 4258–4264.

[11] P.P. Sahay, R.K. Nath, Al-doped zinc oxide thin films for liquid petroleum gas (LPG) sensors, Sensors and Actuators B 133 (2008) 222–227.

[12] X.Y. Xue, Z.H. Chen, L.L. Xing, C.H. Ma, Y.J. Chen, T.H. Wang, Enhanced optical and sensing properties of one-step synthesized Pt–ZnO nanoflowers, Journal of Physical Chemistry C 114 (2010) 18607–18611.

[13] R.K. Joshi, Q. Hu, F. Alvi, N. Joshi, A. Kumar, Au decorated zinc oxide nanowires for CO sensing, Journal of Physical Chemistry C 113 (2009) 16199–16202.

[14] J. Li, H.Q. Fan, X.H. Xia, Multi-layered ZnO nanosheets with 3 D porous architectures: synthesis and gas sensing application, Journal of Physical Chemistry C 114 (2010) 14684–14691.

[15] H.X. Tang, M. Yan, X.F. Ma, H. Zhang, M. Wang, D.R. Yang, Gas sensing behavior of polyvinylpyrrolidone-modified ZnO nanoparticles for triethylamine, Sensors and Actuators B 123 (2006) 324–328.

[16] M.G. Zhao, X.C. Wang, L.L. Ning, H. He, J.F. Jia, L.W. Zhang, X.J. Li, Synthesis and optical properties of Mg-doped ZnO nanofibers prepared by electrospinning, Journal of Alloys and Compounds 507 (2010) 97–100.

[17] J.P. Cheng, Z.M. Liao, D. Shi, F. Liu, X.B. Zhang, Oriented ZnO nanoplates on Al substrate by solution growth technique, Journal of Alloys and Compounds 480 (2009) 741–746.

[18] J.C. Di, H.Y. Chen, X.F. Wang, Y. Zhao, L. Jiang, J.H. Yu, R.R. Xu, Fabrication of zeolite hollow fibers by coaxial electrospinning, Chemistry of Materials 20 (2008) 3543–3545.

[19] S.K. Lim, S.H. Hwang, D. Chang, S. Kim, Preparation of mesoporous In_2O_3 nanofibers by electrospinning and their application as a CO gas sensor, Sensors and Actuators B 149 (2010) 28–33.

[20] S.H. Wei, Y. Yu, M.H. Zhou, CO gas sensing of Pd-doped ZnO nanofibers synthesized by electrospinning method, Materials Letters 64 (2010) 2284–2286.

[21] L. Liu, S.C. Li, J. Zhuang, L.Y. Wang, J.B. Zhang, H.Y. Li, Z. Liu, Y. Han, X.X. Jiang, P. Zhang, Improved selective acetone sensing properties of Co-doped ZnO nanofibers by electrospinning, Sensors and Actuators B 155 (2011) 782–788.

[22] M.G. Zhao, X.C. Wang, L.L. Ning, J.F. Jia, X.J. Li, L.L. Cao, Elcetrospun Cu-doped ZnO nanofibers for H_2S sensing, Sensors and Actuators B 156 (2011) 588–592.

[23] D.J. Qiu, H.Z. Wu, A.M. Feng, Y.F. Lao, N.B. Chen, T.N. Xu, Annealing effects on the microstructure and photoluminescence properties of Ni-doped ZnO films, Applied Surface Science 222 (2004) 263–268.

[24] J.H. Yang, M. Gao, L.L. Yang, Y.J. Zhang, J.H. Lang, D.D. Wang, Y.X. Wang, H.L. Liu, H.G. Fan, Low-temperature growth and optical properties of Ce-doped ZnO nanorods, Applied Surface Science 255 (2008) 2646–2650.

[25] S.J. Pearton, D.P. Norton, K. Ip, Y.W. Heo, T. Steiner, Recent progress in processing and properties of ZnO, Progress in Materials Science 50 (2005) 293–340.

[26] F. Gao, L.X. Tan, Z.H. Wu, X.Y. Liu, Microstructural and optical properties of ZnO/(Ni) thin films prepared by DC magnetron sputtering, Journal of Alloys and Compound 484 (2009) 489–493.

[27] S.S. Nath, M. Choudhury, D. Chakdar, G. Gope, R.K. Nath, Acetone sensing property of ZnO quantum dots embedded on PVP, Sensors and Actuators B 148 (2010) 353–357.

[28] A. Kolmakov, M. Moskovits, Chemical sensing and catalysis by one-dimensional metal-oxide nanostructures, Annual Review of Materials Research 34 (2004) 151–180.

[29] Z.Y. Li, H.N. Zhang, W. Zheng, W. Wang, H.M. Huang, C. Wang, A.G. Macdiarmid, Y. Wei, Highly sensitive and stable humidity nanosensors based on LiCl doped TiO_2 electrospun nanofibers, Journal of the American Chemical Society 130 (2008) 5036–5037.

[30] M. Takata, D. Tsubone, H. Yanagida, Dependence of electrical conductivity of ZnO on degree of sintering, Journal of the American Ceramic Society 59 (1976) 4–8.